A study of the hourly variability of the Urban Heat Island effect in the Greater Athens Area during summer

K. Kourtidis[a], A.K. Georgoulias[a,b], S. Rapsomanikis[a], V. Amiridis[c], I. Keramitsoglou[c], H. Hooyberghs[d], B. Maiheu[d] and D. Melas[e]

[a]Laboratory of Atmospheric Pollution and Pollution Control Engineering of Atmospheric Pollutants, School of Engineering, Democritus University of Thrace, 12 Vas. Sofias str., 67100 Xanthi, Greece. e-mail: kourtidi@env.duth.gr; argeor@env.duth.gr; rapso@env.duth.gr
[b]Department of Meteorology and Climatology, School of Geology, Aristotle University of Thessaloniki, Thessaloniki, Greece.
[c]Institute for Astronomy, Astrophysics, Space Applications and Remote Sensing, National Observatory of Athens (NOA), Athens, Greece. e-mails: ik@noa.gr; vamoir@noa.grmailto:
[d]Flemish Institute for Technological Research (VITO), Boeretang 200,2400 Mol, Belgium. E-mails: hans.hooyberghs@vito.be; bino.maiheu@vito.be
[e]Laboratory of Atmospheric Physics, Physics Dept., Aristotle University of Thessaloniki, Greece. e-mail: melas@auth.gr

[*] Corresponding author. Tel.: +30-25410-79383, Fax: +30-25410-79379.

Abstract

Measurements of air temperature and humidity in the urban canopy layer during July 2009 in 26 sites in Athens, Greece, allowed for the mapping of the hourly spatiotemporal evolution of the Urban Heat Island (UHI) effect. City districts neighboring to the mountains to the east were the hottest during the afternoon, while being among the coolest during the early morning hours. While during the early morning some coastal sites were the hottest, the warm air plume slowly moved to the densely urbanized center of the city until 14:00-15:00, moving then further west, to the Elefsis industrial area in the afternoon. Results from the UrbClim model agree fairly well with the observations. Satellite-derived Land Surface Temperature (LST) data from AATSR, ASTER, AVHRR and MODIS, for the pixels corresponding to ground stations measuring T_{air}, showed that LST can be up to 5 K lower than the respective T_{air} during nighttime, while it can be up to 15 K higher during the rest of the day. Generally, LST during late afternoon as acquired from AATSR is very near to T_{air} for all stations and all days, i.e. the AATSR LST afternoon retrieval can be used as a very good approximation of T_{air}. The hourly evolution of the spatial T_{air} distribution was almost the same during days with NE Etesian flow as in days with sea breeze circulation, indicating that the mean wind flow was not the main factor controlling the diurnal UHI evolution, although it influenced the temperatures attained. No unambiguous observation of the Urban Moisture Excess (UME) phenomenon could be made.

Keywords: urban heat island, urban moisture excess, land surface temperature.

1. Introduction

The impact of urbanization on local climate has been studied for more than a century. Theoretical and experimental studies of thermal contrasts between a city and its surroundings are very abundant in the literature (e.g. Oke, 1979, 1982; Chandler, 1970; Arnfield, 2003). On the other hand, the available literature on moisture contrasts between a city and its surroundings is rather sparse, although the available studies show that urban-rural contrasts exist (Chandler, 1967; Hage, 1975; Ackerman, 1987; Adebayo, 1991; Lee, 1991; Jauregui and Tejeda, 1997; Holmer and Eliasson, 1999; Fortuniak et al., 2006; Liu et al., 2009).

The current work is a study of UHI in the city of Athens, Greece. The urban area of Athens extends beyond the administrative city limits over a land area of 412 km^2. According to a recent census paper of Eurostat (2006), the Athens Larger Urban Zone (LUZ) is the 7^{th} most populated LUZ in the European Union with a population of 4,013,368.

The Athens LUZ, presents characteristics that make it particularly interesting for urban heat island studies. Under given synoptic conditions there are three interacting sets of climatic controls, each operating on different space and time scales. These controls are topography, urban morphology and proximity to the sea. Athens sprawls across the central plain of Attica, often referred to as the Attica Basin, and bound by Mount Egaleo to the west, Mount Parnitha in the north, Mount Penteli in the northeast, Mount Hymettus in the east, and the Saronic Gulf in the southwest (Fig. 1).

Athens enjoys a typical Mediterranean climate, whereby the mountainous northern suburbs experience a somewhat differentiated climatic pattern, with generally lower temperatures. The summer is warm and dry, with July and August being the hottest months. During summer, the city is often subject to sea-breeze circulation (e.g. Helmis et al., 1995; Melas et al., 1998). Summers can be particularly hot and at times prone to smog and pollution episodes. The average daytime maximum temperature for the month of July is 33.5 °C and heat waves are relatively common, occurring generally during the months of July and August, when hot air masses sweep across Greece from the south or the southwest. On such days temperatures can soar over 38 °C. During the summer of 2007, for example, Athens suffered a severe heat wave that lasted for seven days reaching temperatures as high as 46.0 ^{o}C. The all-time high temperature for the metropolitan area of Athens of the order of 48.0 °C was recorded in 1987 in Elefsina, a suburb industrial zone of Athens. Based on a 105-year (1987-2001) surface air temperature record of the National Observatory of Athens, Founda et al. (2004) showed that the annual maximum of the record ranges from 34.7 to 44.1^{0}C.

The city of Athens is characterized by a strong heat island effect, mainly caused by the accelerated industrialization and urbanization during the recentdecades. The Municipality of Athens is a densely built city with a network of high aspect ratio (height/width ratio) streets. The appearance of UHI in the city is mainly linked to limited green and open space areas, lack of water evaporation as well as the high heat storage capacities of building and surface materials, contributing to the magnitude and the duration of the heat wave events. It is also linked to air pollution due to dense traffic and nearby industries, as well as to intense air conditioning.

The study of the urbanization effects on surface air temperature (T_{air}) in Athens started relatively late (Katsoulis and Theoharatos, 1995; Philandras et al., 1999). Several other studies followed, concerned with the occurrence of the UHI effect (Livada et al., 2002), impact on energy consumption (Santamouris et al., 2007), and discomfort index calculation (e.g. Tselepidaki et al., 1992). More recently, satellite-derived LST distribution over Athens was studied (Stathopoulou et al., 2009; Keramitsoglou et al., 2011), while Giannopoulou et al. (2011) mapped the mean monthly T_{air} spatial distribution over Athens for 3 summer months and Giannaros et al. (2013, 2014) modeled the evolution of UHI in Athens with the Weather Research and Forecasting (WRF) model. Very recently, Rapsomanikis et al. (2014) determined the energy and momentum fluxes in the centre of Athens, also using data from the THERMOPOLIS2009 campaign.

The present study aims at filling a gap of previous studies by mapping the summertime T_{air} spatial distribution as well as the water vapor pressure (e) spatial distribution on an hourly basis. This temporal resolution, combined with other ancillary data like wind velocity and direction hourly maps, allows us to study the diurnal course of UHI and UME over Athens as well as the daily differences in the diurnal evolution of UHI created by synoptic factors. We also discuss the effect of wind and the effect of the LST diurnal course on the observed diurnal UHI spatial patterns. The purpose is to improve our understanding of the diurnal UHI evolution in a coastal Mediterranean metropolitan city and to provide data that can help the application of adaptation and mitigation policies.

2. Data and Methods

2.1 In situ observations

Measurements of air temperature in the urban canopy layer were performed during 15-31 July 2009 in 26 sites in Athens (Fig. 1), as part of European Space Agency's (ESA) THERMOPOLIS 2009 campaign (Giannaros et al., 2013; Rapsomanikis et al., 2014). The stations were operated by the Democritus University of Thrace (DUTH, 10 stations), the National Observatory of Athens (NOA, 3 stations), the Hydrological Observatory of Athens, National Technical University of Athens (NTUA, 13 stations) and the Hellenic National Meteorological Service (HNMS, 3 stations). The stations of DUTH and NOA were also measuring relative humidity (RH). DUTH stations were equipped with autonomous HOBO Pro v2 T/RH U23-001 sensors with solar shields. The accuracy is +/-2% for the temperature sensor and +/- 2.5% for the RH one. The sensors have been inter-calibrated and the variability between the sensors was below +/-0.15 ^{o}C for T_{air} and 4% for RH.

To investigate the spatiotemporal evolution of UHI, hourly maps were created by interpolating the data from the 26 stations. The interpolation was performed using the *Delaunay triangulation* method. In mathematics, and computational geometry, a Delaunay triangulation for a set **P** of points in the plane is a triangulation DT(**P**) such that no point in **P** is inside the circumcircle of any triangle in DT(**P**). Delaunay triangulations maximize the minimum angle of all the angles of the triangles in the triangulation and they tend to avoid skinny triangles (see Delaunay, 1934 for details). Compared to any other triangulation of the points, the smallest angle in the Delaunay triangulation is at least as large as the smallest angle in any other. Generally it has been observed that triangulations that lead to good interpolations avoid long and skinny triangles. There is, generally (with the exception of degenerate cases) only one locally optimal triangulation with respect to the angle-vector, namely the Delaunay triangulation (Sibson, 1981). A further property of this triangulation is that the resulting interpolation has lower roughness when compared to other triangulations (Rippa, 1990). Hence, the interpolation performed is the best possible.

The same procedure was followed for the study of the spatiotemporal evolution of UME, where hourly maps were created by interpolating the data from the 13 stations that both T and RH were measured.

Further, a test was performed in which the mean spatial T_{air} was computed using the Delauney triangulation for each hour of the day for three cases:
1. using measurements for the total of the 26 available stations.
2. using data from the 10 DUTH stations only and finally
3. using data from the NTUA and HNMS stations only (16 stations).

Cases 1 and 3 gave almost identical results. Case 2 gives results only for the central; part, since this is where these stations were located, and despite the fact that in this Case much more stations are located in the center, the results for this part of Athens are almost identical with Case 3 where very few stations are located in the center (figures not shown). This gives further credibility to the assumption of a very good interpolation.

Wind velocity and direction data for the period of the campaign were obtained from 9 stations operated by the Hydrological Observatory of Athens, NTUA. The stations use Vector Instruments wind vanes W200P and A100R anemometers on 6 m masts. The wind vane accuracy is +/-3% with a threshold of 0.6 m/s. The anemometer accuracy is +/-2% with a threshold of 0.2 m/s.

2.2 Satellite observations

LST was acquired from a variety of satellite sensors (Table 1). Data from the AVHRR (Advanced Very High Resolution Radiometer) sensor on board NOAA's polar orbiting environmental satellites (POES), MODIS (Moderate Resolution Imaging Spectroradiometer) sensors on board EOS TERRA and AQUA satellites, AATSR (Advanced Along-Track Scanning Radiometer) sensor on board the ENVISAT satellite and ASTER (Advanced Spaceborne Thermal Emission and Reflection Radiometer) sensor on board EOS TERRA were used. The subset of the coarse spatial resolution scenes with a viewing angle larger than 45° was identified and removed, due to the well-documented directional dependence of the LST (e.g. Lagouarde and Irvine, 2008). The images were appropriately processed and the corresponding LST maps for the Greater Athens Area were produced.

2.3 Numerical modeling

UrbClim is an urban climate model designed to model and study the urban heat island effect (UHI) at a spatial resolution of a few hundred meters, described in detail in De Ridder et al. (2015). Briefly, the model downscales large-scale weather conditions to agglomeration-scale and computes the impact of urban development on weather parameters, such as temperature and humidity. UrbClim is composed of a land surface scheme, describing the physics of energy and water exchange between the soil and the atmosphere in the city, coupled to a 3-D atmospheric boundary layer module. The atmospheric conditions far away from the city centre are fixed by meteorological input data, while local terrain and surface data influence the heat fluxes and evaporation within the urban boundaries. The primary output consists of hourly air temperature and apparent air temperature maps with a spatial resolution of 250 m.

The UrbClim model has been subjected to exhaustive validation; Model results have been compared with hourly temperature measurements for, amongst other, London, UK; Bilbao, Spain; and Paris, France (Deridder & Sarkar, 2011; Keramitsoglou et al., 2012).

3. Results and Discussion

The synoptic conditions during the THERMOPOLIS 2009 campaign (15-31 July 2009) were characterized by the presence, in most days, of a low pressure trough over Athens. The Etesian wind system prevented, in most days, the establishment of the local sea breeze circulation. Etesians are strong NE winds over the entire Aegean Sea basin during late summer, created by the presence of a persistent low pressure system over the Arabic Peninsula and a high pressure system over Central Europe (Metaxas, 1977; Tritakis, 1982; Metaxas and Bartzokas, 1994). The setting of the Athens LUZ, with Saronic Gulf to the south, favors during summer the creation of a sea/land breeze circulation (e.g. Helmis et al., 1995; Melas et al., 1998). Days with sea breeze were the 15th, 18th, 19th and 25th of July. On the 17th, the breeze started late in the afternoon, while on the 26th the opposite happened, namely the breeze started early in the morning but a strong Etesian afterwards blocked the local circulation. The rest of the days were days with strong Etesians, resulting in strong NE flow over Athens and no breeze. The period of the measurements started with moderate temperatures which then increased, peaking on the 24-26 July 2009, when they reached 36-40 ^{o}C during daytime throughout the Athens basin. The period from 24 to 26 July 2009 coincided with a Saharan dust intrusion.

3.1 Mean diurnal variation of T_{air}

The T_{air} measurements at 26 sites throughout Athens LUZ allowed for the mapping of the spatiotemporal evolution of the Urban Heat Island in Athens with a temporal resolution of 1 hr for the whole measurement period (see *Video 1* of *Supplement* for a 1-hr step movie of the T_{air} spatial distribution evolution for the whole period of the measurements, 15-31.7.2009, with wind data superimposed). Further, from the mean diurnal variation of each station data, the mean diurnal spatial evolution of UHI was constructed (Fig. 2). To make the diurnal evolution of the spatial UHI variability more clear, absolute T_{air} values were normalized as follows: For each hour i, the mean hourly value T_i for each station was calculated and from these mean values the mean value of all stations T_{mean}. Then, the percent departure of T_i from T_{mean} for each station was calculated, $100(T_i-T_{mean})/T_{mean}$. Maps were then computed using these percent departures and interpolating between stations using the Delaunay triangulation method (see *Section 2* above). Using percent departures from the mean, one can make better visible the UHI variability, as this method highlights areas that are warmer (or cooler) than the overall area mean. Regarding the absolute T_{air} values, they are referenced in Table 2 for 00:00, 6:00, 12:00 and 18:00 UTC (the times referred onwards in the paper are all in UTC). The highest station mean for the period of measurements was around 36 ^{o}C at 12:00 at the DUTH_002 station in the center of the city while the lowest station mean was around 22 ^{o}C at the NTUA_008 station on Mt. Penteli at 00:00 (Table 2).

While during the late night-early morning (21:00-4:00) the coastal and central sites were the hottest, at 5:00-9:00 the west coastal sites were warmer. During 10:00 to 13:00, the central part of the city is warmer. In the afternoon, 15:00-20:00, a “warm air plume” extends from the center all the way to the west of Athens LUZ towards the industrial area north of Elefsis Bay (Fig.2). It is also apparent (Fig. 2) that the NE part of the basin, near or at Mt. Penteli, is cooler than the rest of the Attica basin during the whole course of the day. Another pool of cool air exists between 4:00 and 8:00 in the early morning at the west of the basin and a less pronounced one between 18:00 in the afternoon and 4:00 in the early morning at the east of the basin.

While Fig. 2 represents a mean diurnal pattern of deviations from the area mean, it is interesting to examine the diurnal evolution during each day (movie created from hourly T_{air} and wind data for the whole campaign period available in *Video 1* of *Supplement*). In all days (15-31.7.2009), the same consistent spatial pattern of the diurnal evolution of T_{air} is clear, with only small deviations, despite the fact that there were days of NE Etesian flow, days with sea breeze circulation and days of SW flow conditions: In the morning, coastal sites exhibit higher temperatures. At around noon, central Athens has higher T_{air}, while as the afternoon proceeds the higher T_{air} values extend toward the north/northwest from the center. At midnight, coastal and central sites have higher T_{air}. That the hourly evolution of the spatial T_{air} distribution was almost the same during days with NE Etesian flow as in days with sea breeze circulation, indicates that the mean wind flow is not the main factor controlling the diurnal UHI evolution in Athens during campaign conditions.

To help the reader with the interpretation of the results above, and also give an indication of the absolute values of the temperature and their diurnal evolution at different UHI zones of the city, along with the information provided in Table 2, Fig. 3 depicts the mean diurnal variation of the absolute values of T_{air} at four different UHI zones of the city: The center, the coast, the NE and the NW.

Very few studies exist for the T_{air} UHI of Athens. Katsoulis and Theoharatos (1995) studied the impact of Athens expansion 1961-1982 on the air temperatures in Athens and the differences between the city and its surroundings. The Livada et al. (2002) study of Athens UHI dealed mainly with the urban-rural temperature differences as well as climatological statistics. Hence, the present study significantly enhances our present understanding of the UHI over Athens and is the first one to focus on the hourly spatial variability of Athens UHI. As such, it can help the application of mitigation and adaptation policies. For example, we are currently working in combining the data of Fig. 2 with population, energy use and other ancillary data, to estimate the diurnal spatial evolution of air-conditioning energy demand over the Athens LUZ.

3.2 LST satellite data and their relation to T_{air}

Satellite LST values for the pixels corresponding to ground stations measuring T_{air} were acquired from five spaceborne sensors, namely AVHRR, MODIS TERRA, MODIS AQUA, ASTER, and AATSR. For each station, timeseries of T_{air} and the corresponding LST (i.e. the LST for the satellite pixel where each station lies within) show that, generally (Fig. 4):The satellite-derived LST from AATSR, ASTER, AVHRR and MODIS for the pixels corresponding to the T_{air} ground stations can be up to 5 K lower than the respective T_{air} during late afternoon/nighttime, although in many cases the difference (LST-T_{air}) is much smaller. On the other hand, during the daytime, LST can get up to 15 K higher than the respective T_{air}. This is also in agreement with diurnal LST-T_{air} differences observed in Madrid in a recent study of the impact of overpass time on evaluation of UHI effects (Sobrino et al., 2012), and hence it shows that these diurnal LST-Tair differences may be a ubiquitous feature of urban areas in Mediterranean climates.

However, the late afternoon (overpass time around 20:00 UTC) AATSR LST retrievals agree very well with Tair for all the stations and all the days, i.e. for Athens the AATSR LST late afternoon retrieval is a very good approximation of T_{air}. The same holds for the AVHRR LST late afternoon retrievals. Reconstruction of T_{air} from LST remains a challenge. However, the results from Athens above, which confirm the recent results from Madrid of Sobrino et al. (2012), imply that it is possible to reconstruct the spatial evolution of the diurnal variation of the T_{air} UHI over Athens during summer without actually measuring T_{air}. This could be done using afternoon LST AVHRR observations (since AATSR data on ENVISAT are no longer available due to ENVISAT decommissioning in 2013) as proxy for T_{air} at the overpass time and the robust statistical relationship that exists between afternoon T_{air} (at overpass time) and T_{air} in other times of the day. This relationship can be easily defined from the observed mean diurnal variation at each station. The MODIS late afternoon and early morning data agree also fairly well (although not as good as AATSR and AVHRR) with T_{air} for most stations and most days, in all cases the difference being < 4 K. Retalis et al. (2010) also compared MODIS AQUA afternoon LST data with T_{air} data from several stations in Athens during the June 2007 heat wave and found differences generally within the 3 to 5 K range, in general agreement with our results. As ASTER revisit time is not daily but 16 days, and further ASTER overpasses Athens at around 9:20 UTC, i.e. 11:20 local time, when the difference between LST and T_{air} is maximum, it is not suitable for deriving daily T_{air}, although its spatial resolution at 90 m (Table 1) is much better that the other sensors (1.1 km). For some pixels, we had concurrent to ASTER, MODIS and AVHRR acquisitions. As can be seen in Fig. 4, it is worth noting that the different spatial resolution results most times in different LST for co-located pixels (Fig. 4a, b, c, g, h) while sometimes (Fig. 4d) not. In any case, all results showed that at the time of ASTER overpass the two parameters (LST and T_{air}) differ the most. It is to be stressed, that discrepancies between LST retrievals from different satellite sensors are mainly due to the effects induced by the different spatial scales, as well as, the not-matching viewing direction of the sensors. Recent results obtained for Athens (Sismanidis et al., 2015), indicate that many factors may affect the performance of any downscaling algorithm, rugged terrain and land cover being important factors for discrepancies between scales and sensors. As a general remark, the nighttime comparisons show better agreement since the absence of shadows lessens the effects induced by the LST directional anisotropy (Trigo et al., 2008). Therefore, even coincident measurements of LST from different sensors are in practice not comparable.

3.3 Case studies

We will now proceed to examine the diurnal evolution of the UHI spatial variability in three case studies, the one typical for summer days with sea breeze circulation (15th of July, case denoted BRE hereafter), the other typical of days of Etesian winds with NE mean synoptic flow (22nd of July, ETE) and the last for a day with very high temperatures, NE mean synoptic flow, sea breeze circulation and Saharan dust transport (25th of July, SAH).

3.3.1 Case study #1, BRE, sea breeze circulation: July 15, 2009

During this day of sea breeze local circulation, a strong W flow prevails over Saronicos Gulf, while in the other parts of the basin, except the northwestern ones, the wind velocity is very low. As the daytime starts and proceeds, a sea breeze with S flow is gradually established, starting early in the morning over the parts of the basin that are closer to the coast (8:00-10:00) and suppressing then gradually the N-NE flow that exists over the northern parts. The N-NE flow over these parts does not disappear completely nor is it reversed to S flow; it just weakens considerably until 18:00. It is subsequently reestablished between 18:00-20:00 over the northern/central part of the basin and by 21:00 also the southern parts and the coast are under Northern flow.

In the central parts of the basin, most of the day, the winds are weak, 0-1 m s^{-1}, while at the coast and the NE parts they are very vivid, up to 2.5 m s^{-1}.

The MODIS satellite LST acquisitions shortly after midnight (00:15) show that the city center is the hottest, while around noon (13:30) the warmest city districts are the ones at the NW, namely the industrial area north of Elefsis Bay (Fig. 5). This is a typical industrial area, with low buildings, sparse vegetation cover and largely covered by bare soil.

At 00:00, the coastal sites are the hottest. At 8:00, the city center gets warmer, while at 11:00-16:00 the whole area except the cooler NE have the same temperatures. At 17:00-20:00 the warmest city districts extend from the center N to the industrial area of Elefsis at the NW, apparently T_{air} following with a lag LST. During the late nighttime, the center and the coast are the warmest parts of the city (Fig. 5 and *Video 1* of *Supplement*).

3.3.2 Case study #2, ETE, NE mean synoptic flow: July 21, 2009

During this day of Etesian synoptic flow, in most parts of the basin the flow is NNE. The eastern part exhibits a different flow regime, with winds fluctuating between W and NW at different times of the day and different western stations. In most parts of the basin and most of the day the winds are 1.5-2 m s^{-1}.

MODIS satellite LST acquisitions shortly after midnight (00:15) show that the city center is the hottest, while around noon (13:30) the warmest city districts are the ones at the NW, namely the industrial area north of Elefsis Bay (Fig. 6). Compared with the LST of Case study #1 (sea breeze circulation), ETE LST is higher around midnight while it is somewhat lower during noon, the general spatial pattern being the same in both cases.

Regarding the evolution of surface air temperature, at 00:00, the coastal sites and the center are the hottest. At 8:00, the coastal sites get warmer, while at 11:00-15:00 the center is warmer while at 17:00-19:00 the warmest city districts are the ones at the center as well as the ones at the industrial area at the NW, apparently T_{air} following with a lag LST, as in Case study #1. During the late nighttime, the center and the coast are the warmest parts of the city (Fig. 6 and *Video 1* of *Supplement*).

3.3.3 Case study #3, SAH, very high air temperatures, NE mean synoptic flow, sea breeze circulation and Saharan dust transport: July 25, 2009

On the 24^{th}, 25^{th} and 26^{th} of July, the air temperatures soared throughout the Athens basin, reaching 35-40 ^{o}C during the daytime. The synoptic flow over Athens was NE, and the onset of high air T coincided with the intrusion of a Saharan dust plume. Back-trajectory calculations show that the dust plume originated from the Sahara 4 days ago and was then transported over the Iberian peninsula and after travelling to the east the following dates it entered the Balkans from the NE. The dust plume arrived over Athens on the morning of the 24^{th} at an altitude of 2.3-4 km and the following days it extended throughout the boundary layer and up to 4 km altitude. On the 25^{th} of July, which we will examine here, the Saharan dust plume extended throughout the boundary layer, the Etesian system created a NE synoptic flow over the Athens basin and from 7:00 in the morning to 20:00 in the late afternoon a strong sea breeze with wind velocities up to 2.5 m s^{-1} persisted over the whole basin, overriding the mean synoptic flow.

MODIS satellite LST acquisitions in the morning show that at 10:48 the city center is hot but the warmest city districts extend from the center N to the industrial area of Elefsis at the NW, while around noon (13:30) the city center has cooled down and the warmest city districts are the ones at the industrial area at the NW (Fig. 7). At 21:30 at night, the whole city center is warmer than the industrial area at the NW. Compared with the LST of Case studies #1 (sea breeze circulation) and #2 (Etesian NE flow), during the midday (where in all three cases an LST acquisition was made) the general LST spatial pattern is the same in all cases.

Regarding the evolution of surface air temperature, early in the morning the coastal sites and the center are the hottest. From 8:00 to 19:00, the warmest city districts extend from the center N to the NW. The differences are the largest at 18:00. During the late nighttime, the center and the coast are the warmest parts of the city (Fig. 7 and *Video 1* of *Supplement*).

Overall, it can be said that there are not large differences in the spatiotemporal evolution of UHI over Athens in summer under different meteorological regimes (Figs. 5 to 7), indicating, as discussed above and as it becomes evident from the case studies presented, that the mean wind flow is not the main factor controlling the diurnal UHI evolution in Athens during summertime, although it influences the temperatures attained. It appears, that thermodynamical (i.e. factors pertaining to the surface radiation balance, such as surface albedo, emissivity, building storage heat) rather than dynamical factors exert a major influence in the evolution of the studied UHI. Indeed, the building storage heat fluxes are very large over Athens, reaching 155 W/m^2 during the day and -125 W/m^2 during night, as determined recently by Rapsomanikis et al. (2014). Also, high LST over Athens results in large upwelling longwave radiative fluxes (on average 510 W/m^2 (Rapsomanikis et al., 2014).

3.4 Humidity

Several studies have shown that humidity differences exist between urban and rural areas (e.g. Jauregui and Tejeda, 1997). Many studies show urban areas to be moister than their surroundings (e.g. Fortuniak et al., 2006; Kuttler et al., 2007), also in Greece (Giannaros et al., 2012) and the urban moisture excess (UME) has been shown to influence the radiative balance and enhance UHI (Holmer and Eliasson, 1999). Cicek and Turkoglu (2009) report positive UME in a semi-arid climate. Holmer and Eliasson (1999) found positive UME, especially during nighttime, in the northern climate of Goeteborg, Sweden. Adebayo (1991) reports that at a tropical city in Nigeria, water vapor pressure was lower in the city than in rural surroundings. Unkasevic et al. (2001) found positive or negative differences in Belgrade, depending on season and time of the day.

The RH and T measurements at 13 of the 26 sites allowed for the mapping of the spatiotemporal evolution of the Urban Moisture Excess (UME) in Athens with a temporal resolution of 1 hr for the whole measurement period. For this, the absolute water vapor pressure e was calculated from the T and RH measurements (Bolton, 1980).

Further, from the mean diurnal variation of each station data, the mean diurnal spatial evolution of UME was constructed (Fig. 8). To make the diurnal evolution of the spatial UME variability clearer, absolute water vapor pressure e values were normalized as follows: For each hour i, the mean hourly value e_i for each station was calculated and from these mean values the mean value of all stations e_{mean}. Then, the percent departure of e_i from e_{mean} for each station was calculated, $100(e_i - e_{mean})/e_{mean}$. Maps were then computed using these percent departures and interpolating between stations using the Delaunay triangulation method (see *Section 2* above). Using percent departures from the mean can make better visible the UME variability, as it highlights areas that are more moist (or more dry) than the overall area mean. Regarding the absolute RH and e values, they are referenced in Table 3 for 00:00, 6:00, 12:00 and 18:00. The lowest station RH mean for the period of measurements was around 23% at 12:00 at the DUTH_002 station in the center of the city while the highest station mean was around 53% at the NOA2_002 station on Mt. Penteli at 00:00 (Table 3).

Higher water vapor values are present in all times of the day near the city center (i.e. a positive UME is observed); however, station NOA1_1 which exhibits the highest water vapor values (mean up to 18 mbar at 18:00, Table 3) was placed at a vegetated hill near the city center (Pnyx hill) and is therefore responsible for the observed UME. The lowest water vapor values were observed at station NOA3_003 at the eastern part of the LUZ (Goudi district) at 06:00 and 12:00 (down to 13.47±2.42 mbar) and at station DUTH_007 at the northeastern part of the LUZ at 00:00 and 18:00 (down to 13.57±2.40 mbar).

The diurnal variation of e is not very pronounced in stations within the dense urban fabric (Fig. 9 top and bottom left) while at stations in vegetated areas e is higher during the daytime, possibly due to evapotranspiration from vegetation (Fig. 9 bottom right).

These results add to the evolving recent literature on urban moisture, mentioned in the beginning of this paragraph. As with some of the mentioned studies, UME has not been observed unambiguously. Further, UME has not been observed during any part of the day. In future studies, it will be worthwhile to study urban moisture over Athens not only at ground level, but also aloft, as a recent study for Shangai shows moisture transport from the surface aloft, due to ascending air motions (Kang et al., 2014). Given the complex topography of Athens, and the complex and variable local circulation patterns, resulting from the combined result of the thermally induced local circulation systems superposed on the mesoscale and synoptic wind field (Batchvarova and Gryning, 1998; Melas et al., 1998; Ziomas, 1998), such future studies would help elucidate the horizontal and vertical transport and fate of water vapour over the city.

3.5 Comparison with model results

The experimental T_{air} results were compared with VITO's UrbClim model, an urban climate model designed to model and study the urban UHI at a spatial resolution of a few hundred meters (De Ridder et al., 2014).

The meteorological input for the current study was taken from the large-scale (70 km resolution) ERA-interim re-analysis data set of the European Centre for Medium-Range Weather Forecasts (ECMWF) (Dee et al., 2011). The terrain input consists of the spatial distribution of land use types, the degree of covering of the soil by artificial structures such as buildings and roads, the vegetation cover fraction with a spatial resolution of 250 m, and detailed elevation data. These quantities were all taken from publicly available data sets, namely the 2006 CORINE land cover data for Europe (EEA, 2007), the European Environment Agency (EEA) soil sealing data (Maucha et al., 2010), the Normalized Difference Vegetation Index acquired by the MODIS instrument on the TERRA satellite (Huete et al., 1999) and the Global Multi-resolution Terrain Elevation Data (GMTED) of the U.S. Geological Survey (USGS), respectively.

The mean T_{air} from the period of the THERMOPOLIS campaign (15-31 July 2009) as measured in the 25 deployed stations was compared with the mean T_{air} from the same period as computed in the respective 250 m grid points by the UrbClim model (one of the stations lies outside the modeled area and was not considered). The spatial variation of T_{air} is reproduced quite well from the model (Fig. 10), with a correlation of r^2=0.78 and a RMSE error of around 1 ^{0}C. Although there is a good linear relationship between the modeled and the measured data, the modeled data are, in general, slightly too low. Model results are shown in Figure 11, in which the mean diurnal cycle of the air temperature in the Athens area is shown. Less agreement is observed in the diurnal variation of temperature differences between the measured (Fig. 2) and the modeled (Fig. 11) T_{air}. The error statistics that are observed in this study are in line with other validations of UrbClim. Correlation coefficients between 0.7 and 0.8, and RMSE-values varying from 0.9 °C to 1.2 °C have previously been obtained for Berlin, London, Bilbao, Ghent and Antwerp (De Ridder et al, 2015). In all these cases, the spatial variation is also reproduced more accurately than the diurnal cycle.

Apart from the present study, only two modeling studies of Athens UHI have been published (Giannaros et al., 2013, 2014). These employ the mesoscale WRF model. The model in Giannaros et al. (2014) employs the mesoscale meteorological WRF model, the Noah land surface model and a statistical downscaling mask to increase spatial resolution and was implemented for 1.5 month during summer 2010. The model had a mean bias error for the mean, min and max daily temperatures of 0.36 K, -0.79 and 1.33 K, respectively, and a root mean squared error of 1.19 K, 1.66 K and 2.05 K, respectively. The same model without the downscaling mask was employed also in Giannaros et al. (2013), for 2 days of summer 2009, where the model had a mean bias error of -0.23 K and a root mean squared error of 1.33 K. The UrbClim model in the present study uses different parameterizations, is found to perform satisfactorily for Athens, and enhances the sparse literature of modeling studies for Athens UHI.

4. Conclusions

In this study, we studied the hourly evolution of summertime UHI in a large Mediterranean coastal urban area, the city of Athens, which has a population of over 4 million and covers an area of 412 km^2. City districts neighboring to the mountains to the east of Athens LUZ were the hottest during the afternoon, while being among the coolest during the early morning hours. While during the early morning some coastal sites were the hottest, the hot air plume slowly moved to the densely urbanized center of the city until 14:00-15:00, moving then further west to the industrial area north of Elefsis Bay during the afternoon.

The hourly evolution of the spatial T_{air} distribution was almost the same during days with NE Etesian flow as in days with sea breeze circulation, indicating that the mean wind flow was not the main factor controlling the diurnal UHI evolution, although it influenced the temperatures attained. It appears, that thermodynamical (i.e. factors pertaining to the surface radiation balance, such as building storage heat) rather than dynamical factors excert a major influence in the evolution of the studied UHI.

Satellite-derived Land Surface Temperature (LST) data from AATSR, ASTER, AVHRR and MODIS for the pixels corresponding to ground stations measuring T_{air}, showed that LST can be up to 5 K lower than the respective T_{air} during nighttime, while it can be up to 15 K higher during the rest of the day. Generally, LST during late afternoon as acquired from AATSR (overpass time around 20:00 UTC) is the same as T_{air} for all stations and all days, i.e. for Athens the AATSR LST late afternoon retrieval can be used as a very good approximation of T_{air}. As these results are in agreement with diurnal LST-T_{air} differences observed in Madrid in a recent study of the impact of overpass time on evaluation of UHI effects (Sobrino et al., 2012), it shows that these diurnal LST-Tair differences may be a ubiquitous feature of urban areas in Mediterranean climates.

No unambiguous observation of the Urban Moisture Excess (UME) phenomenon in the Athens LUZ could be made. In future studies, it will be worthwhile to study urban moisture over Athens not only at ground level, but also aloft. Given the complex topography of Athens, and the complex and variable local circulation patterns, resulting from the combined result of the thermally induced local circulation systems superposed on the mesoscale and synoptic wind field, such future studies would help elucidate the horizontal and vertical transport and fate of water vapour over the city.

Acknowledgements

This work has been funded by the European Space Agency (ESA) under the THERMOPOLIS 2009 campaign (ESA Contract No.22693/09/I-EC). The authors would also like to thank all the teams that participated in the THERMOPOLIS campaign. Part of the surface meteorological dataset (wind velocity and direction data as well as some surface temperature data) was obtained from the Hydrological Observatory of Athens, NTUA (http://hoa.ntua.gr). The modelling work described in this paper has received funding from the European Community's 7th Framework Programme under Grant Agreements Nos. 308497 (RAMSES) and 308299 (NACLIM), and from the Belgian Science Policy Office through its Science for a Sustainable Development Programme under contract SD/CS/041 (MACCBET).

References

Ackerman, B., 1987. Climatology of Chicago area urban-rural differences in humidity. J. Climate Appl. Meteorol. 26, 427-430.

Adebayo, Y.R., 1991. Day-time effects of urbanization on relative humidity and vapour pressure in a tropical city. Theor. Appl. Climatol. 43, 17-30.

Arnfield, A.J., 2003. Two decades of urban climate research: A review of turbulence, exchanges of energy and water, and the urban heat island. Int. J. Climatol. 23, 1-26.

Batchvarova, E., Gryning, S.-E., 1998. Wind climatology, atmospheric turbulence and internal boundary-layer development in Athens during the MEDCAPHOT-TRACE experiment. Atmos. Environ. 32, 2055-2069.

Bolton, D., 1980. The computation of equivalent potential temperature. Mon. Weather Rev. 108, 1046–1053.

Chandler, T.J., 1967. Absolute and relative humidities in towns. Bull. Amer. Meteorol. Soc. 48, 394-399.

Chandler, T.J., 1970. Selected bibliography on urban climate. Technical Note no. 155, WMO no. 276, World Meteorological Organisation, Geneva.

Cicek, I., Turkoglu, N., 2009. The effects of urbanization on water vapour pressure in a semi-arid climate. Theor. Appl. Climatol. 95, 125–134

Davenport, A.G., Grimmond, C.S.B., Oke, T.R., Wieringa, J., 2000. Estimating the roughness of cities and sheltered country. Proc. 12th Conf. on Applied Climatology, Asheville, NC, American Meteorological Society, Boston, pp. 96-99.

Dee, D. P., Uppala, S. M., Simmons, A. J., Berrisford, P., Poli, P., Kobayashi, S., Andrae, U., Balmaseda, M. A., Balsamo, G., Bauer, P., Bechtold, P., Beljaars, A. C. M., van de Berg, L., Bidlot, J., Bormann, N., Delsol, C., Dragani, R., Fuentes, M., Geer, A. J., Haimberger, L., Healy, S. B., Hersbach, H., Hólm, E. V., Isaksen, L., Kållberg, P., Köhler, M., Matricardi, M., McNally, A. P., Monge-Sanz, B. M., Morcrette, J.-J., Park, B.-K., Peubey, C., de Rosnay, P., Tavolato, C., Thépaut, J.-N. and Vitart, F., 2011. The ERA-Interim reanalysis: configuration and performance of the data assimilation system. Q. J. R. Meteorol. Soc. 137, 553–597.

Delaunay, B., 1934. Sur la sphère vide. Izvestia Akademii Nauk SSSR, Otdelenie Matematicheskikh i Estestvennykh Nauk, 7, 793–800.

De Ridder, K., Sarkar, A., 2011. The urban heat island intensity of Paris: a case study based on a simple urban surface parameterisation. Boundary-Layer Meteorol. 138, 511–520.

De Ridder, K., Lauwaet, D., Maiheu, B., 2015. UrbClim – a fast urban boundary layer climate model. Urban Climate 12, 21-48.

EEA (European Environment Agency), 2007. CLC 2006 technical guidelines. EEA Technical Report No 17/2007.

Eurostat, 2006. City statistics - Urban audit. European Commission, Brusselles.

Fortuniak, K., Klysik, K., Wibig, J., 2006. Urban-rural contrasts of meteorological parameters in Lodz. Theoretical and Applied Climatology 84, 91–101.

Founda, D., Papadopoulos, K.H., Petrakis, M., Giannakopoulos, C., Good, P., 2004. Analysis of mean, maximum and minimum temperature in Athens from 1897 to 2001 with emphasis on the last decade: Trends, warm events and cold events. Global and Planetary Change 44, 27-38.

Giannaros, T.M., Melas, D., 2012. Study of the urban heat island in a coastal Mediterranean city: The case study of Thessaloniki, Greece. Atmos. Res. 118, 103-120.

Giannaros, T.M., Melas, D., Daglis, I.A., Keramitsoglou, I., Kourtidis, K., 2013. Numerical study of the urban heat island over Athens (Greece) with the WRF model. Atmos. Environ. 73, 103-111.

Giannaros, T.M., Melas, D., Daglis, I.A., Keramitsoglou, I., 2014. Development of an operational modeling system for urban heat islands: An application to Athens, Greece. Natural Hazards and Earth System Sciences 14, 347-358.

Giannopoulou, K., Livada, I., Santamouris, M., Saliari, M., Assimakopoulos, M., Caouris, Y.G., 2011. On the characteristics of the summer urban heat island in Athens, Greece. Sustainable Cities and Society 1, 16–28.

Hage, K.D., 1975. Urban-rural humidity differences. J. Appl. Meteorol. 14, 1277-1283.

Helmis, C.G., Papadopoulos, K.H., Kalogiros, J.A., Soilemes, A.T., Asimakopoulos, D.N., 1995. Influence of background flow on evolution of Saronic gulf sea breeze. Atmos. Environ. 29B, 3689–3701.

Holmer, B., Eliasson, I., 1999. Urban-rural vapour pressure differences and their role in the development of urban heat islands. Int. J. Climatol. 19, 989–1009.

Huete, A., Justice, C., Van Leeuwen, W., 1999. MODIS vegetation index (MOD13). Algorithm theoretical basis document, Version 3, University of Arizona, Tuscon, U.S.A.

Jauregui, E., Tejeda, A., 1997. Urban-rural humidity contrasts in Mexico city. Int. J. Climatol. 17, 187-196.

Kang, H.-Q., Zhu, B., Zhu T., Sun, J.-L., Ou, J.-J., 2014. Impact of megacity Shanghai on the Urban Heat-Island effects over the downstream city Kunshan. Boundary-Layer Meteorol. 152, 411–426.

Katsoulis, B.D., Theoharatos, G.A., 1995. Indications of the urban heat island in Athens, Greece. J. Climate Appl. Meteorol. 24, 1296–1301.

Keramitsoglou, I., Kiranoudis, C.T., Ceriola, G., Weng, Q., Rajasekar, U., 2011. Identification and analysis of urban surface temperature patterns in Greater Athens, Greece, using MODIS imagery. Remote Sensing of Environment 115, 3080–3090.

Keramitsoglou, I., Daglis, I.A., Amiridis, V., Chrysoulakis, N., Ceriola, G., Manunta, P., Maiheu, B., De Ridder, K., Lauwaet, D., Paganini, M., 2012. Evaluation of satellite-derived products for the characterization of the urban thermal environment. J. Appl. Remote Sens. 6, 061704.

Kuttler, W., Weber, S., Schonnefeld, J., Hesselschwerdt, A., 2007. Urban/rural atmospheric water vapour pressure differences and urban moisture excess in Krefeld, Germany. Int. J. Climatol. 27, 2005-2015.

Lagouarde, J.-P., Irvine, M., 2008. Directional anisotropy in thermal infrared measurements over Toulouse city center during the CAPITOUL measurement campaigns: First results. Meteorol. Atmos. Phys. 102, 173–185.

Lee, D.O., 1991. Urban-rural humidity differences in London. Int. J. Climatol. 11, 577-582.

Livada, I., Santamouris, M., Niachou, K., Papanikolaou, N., Mihalakakou, G., 2002. Determination of places in the great Athens area where the urban heat island effect is observed. Theor. Appl. Climatol. 71, 219-230.

Liu, W., You, H., Dou, J., 2009. Urban-rural humidity and temperature differences in the Beijing area. Theoretical and Applied Climatology 96, 201–207.

Maucha, G., Büttner, G., Kosztra, B., 2010. European validation of GMES FTS Soil Sealing Enhancement data. European Topic Centre Land Use and Spatial Information (ETC-LUSI) report, Institute of Geodesy, Cartography and Remote Sensing (FÖMI), Budapest, Hungary.

Melas, D., Ziomas, I., Klemm, O., Zerefos, C.S., 1998. Anatomy of the sea-breeze circulation in Athens area under weak large-scale ambient winds. Atmos. Environ. 32, 2223–2237.

Metaxas, D.A., 1977. The interannual variability of the Etesian frequency as a response of atmospheric circulation anomalies. Bulletin of the Hellenic Meteorol. Soc. 2, 5, 30–40.

Metaxas, D., Bartzokas, A., 1994. Pressure covariability over the Atlantic, Europe and N. Africa. Application: centers of action for temperature, winter precipitation and summer winds in Athens, Greece. Theor. Appl. Clirnatol. 49, 9-18.

Oke, T.R., 1979. Review of urban climatology, 1973-1976. Technical Note no. 169, WMO no. 539, World Meteorological Organisation, Geneva.

Oke, T.R., 1982. Bibliography of urban climate 1977-1980. WCP-45, World Meteorological Organisation, Geneva.

Oke, T.R., 2006. Initial Guidance to obtain representative meteorological observations at urban sites. Instruments and observing methods Report No. 81, WMO/TD-No. 1250, World Meteorological Organisation, Geneva.

Philandras, C.M., Metaxas, D.A., Nastos, P.Th., 1999. Climate Variability and Urbanization in Athens. Theor. Appl. Climatol. 63, 65-72.

Rapsomanikis, S., Trepekli, A., Loupa, G., Polyzou, C., 2014. Vertical Energy and Momentum Fluxes in the Centre of Athens, Greece During a Heatwave Period (Thermopolis 2009 Campaign). Boundary-Layer Meteorol. DOI 10.1007/s10546-014-9979-2.

Retalis, A., Paronis, D., Lagouvardos, K., Kotroni, V., 2010. The heat wave of June 2007 in Athens, Greece—Part 1: Study of satellite derived land surface temperature. Atmos. Res. 98, 458–467.

Rippa, S., 1990. Minimal roughness property of the Delaunay triangulation. Computer Aided Geometric Design 7, 489-497.

Santamouris, M., Paraponiaris, K., Mihalakakou, G., 2007. Estimating the ecological footprint of the heat island effect over Athens, Greece. Climatic Change 80, 265–276.

Sibson, R., 1981. A brief description of natural neighbor interpolationts. In: *Interpreting Multivariate Data*, Ed. V. Barnett, Chichester, 21-36, John Wiley.

Sismanidis, P., Keramitsoglou, I., Kiranoudis, C.T., 2015. Evaluating the Operational Retrieval and Downscaling of Urban Land Surface Temperatures. IEEE Geoscience and Remote Sensing Letters (In Press). doi: 10.1109/LGRS.2015.2397450.

Sobrino, J.A., Oltra-Carrió, R., Sòria, G., Bianchi, R., Paganini, M., 2012. Impact of spatial resolution and satellite overpass time on evaluation of the surface urban heat island effects. Remote Sensing of Environment 117, 50–56.

Stathopoulou, M., Synnefa, A., Cartalis, C., Santamouris, M., Karlessi, T., Akbari, H., 2009. A surface heat island study of Athens using high-resolution satellite imagery and measurements of the optical and thermal properties of commonly used building and paving materials. Int. J. of Sustainable Energy 28, 1-3, 59-76.

Trigo, I.F., Monteiro, I.T., Olesen, F., Kabsch, E., 2008. An Assessment of Remotely Sensed Land Surface Temperature. J. Geophys. Res. 113, D17, D17108, doi:10.1029/2008JD010035.

Tritakis, B.P., 1982. Etesians distribution within the Bartel rotations no. 1938–2027 (1975–1981). Geophys. Res. Lett. 9, 1225–1226.

Tselepidaki, I., Santamouris, M., Moustris, C., Poulopoulou, G., 1992. Analysis of the summer discomfort index in Athens, Greece, for cooling purposes. Energy and Buildings 18, 51-56.

Unkasevic, M., Jovanovic, O., Popovic, T., 2001. Urban-suburban/rural vapour pressure and relative humidity differences at fixed hours over the area of Belgrade city. Theor. Appl. Climatol. 68, 67-73.

Wieringa, J., 1992. Updating the Davenport roughness classification. Journal of Wind Engineering and Industrial Aerodynamics 41-44, 357-368.

Ziomas, I., 1998. The Mediterranean campaign of photochemical tracers-transport and chemical evolution (MEDCAPHOT-TRACE): An outline. Atmos. Environ. 32, 2045-2053.

Table 1. Characteristics of the satellite sensors used for LST acquisitions.

Sensor	Ground resolution at nadir (km)	Revisit frequency	Approx. Athens overpass time (U
ASTER	0.09	16 days	9:30
AATSR	1.1	Twice daily	9:00 and 20:00
MODIS TERRA and AQUA	1.1	Twice daily each	Variable
AVHRR	1.1	3 to 4 times daily, depending on NOAA platforms operational	Variable

Table 2. Mean air temperatures T_{air} (^{o}C) and their corresponding standard deviations (±1σ) for 00:00, 06:00, 12:00 and 18:00 UTC for the period 15-31 July 2009 for 26 stations in the Athens LUZ. Station coordinates are also given. For each time, the highest and lowest T_{air} are highlighted with dark and light grey shadow, respectively.

Station	Latitude (deg N)	Longitude (deg E)	00:00	06:00	12:00	18:00
DUTH_001	38.0226	23.8334	26.02±1.29	29.32±2.23	32.29±2.44	28.38±1.75
DUTH_002	37.9965	23.7330	28.96±1.19	29.50±1.29	35.98±1.78	31.24±1.27
DUTH_003	38.0279	23.8174	26.46±1.61	27.91±1.86	33.28±2.43	28.81±2.06
DUTH_004	37.9698	23.7488	26.84±1.20	28.75±1.79	34.19±2.07	29.55±1.60
DUTH_005	37.9260	23.7124	27.78±1.05	29.23±1.15	33.76±1.64	30.13±1.47
DUTH_006	37.9569	23.6575	28.19±1.09	31.90±1.73	34.03±1.61	30.27±1.42
DUTH_007	38.0553	23.8129	24.36±1.28	28.12±2.35	31.80±2.48	27.40±1.76
DUTH_OA1	37.9816	23.7810	24.94±1.23	27.47±1.74	33.05±2.35	29.10±1.76
DUTH_OA2	37.9627	23.7564	27.27±1.57	28.45±1.71	33.24±2.09	29.57±1.56
DUTH_OA3	37.9627	23.7564	27.44±1.65	27.80±1.66	32.71±2.33	29.62±1.74
HNMS_001	38.0497	23.6600	25.76±1.09	23.87±1.16	33.92±2.93	32.18±2.02
HNMS_002	37.8997	23.7433	26.76±1.25	25.32±1.51	33.56±1.58	32.41±1.38
HNMS_003	38.0669	23.5500	26.87±1.52	25.80±1.57	33.45±2.02	32.59±2.08
NOA1_001	37.9720	23.7180	27.41±1.34	30.30±1.58	35.58±2.42	29.75±1.56
NOA2_002	38.0473	23.8650	23.70±2.29	26.08±2.57	29.42±2.44	24.73±1.94
NOA3_003	37.9880	23.7750	25.74±1.14	28.67±2.29	32.61±2.46	28.57±1.76
NTUA_001	37.9771	23.7869	22.74±1.84	29.84±2.43	34.72±2.47	27.16±1.43
NTUA_002	38.1066	23.7339	24.93±1.37	29.52±2.32	33.33±2.61	27.34±1.74
NTUA_003	37.9419	23.5871	26.79±1.06	28.65±1.23	32.46±1.90	28.32±0.97
NTUA_004	37.8988	23.7234	27.04±0.97	28.79±1.14	32.56±2.33	29.37±1.26
NTUA_005	37.9183	23.7610	25.97±1.73	28.86±1.95	33.98±2.07	28.24±1.83
NTUA_006	38.1229	23.5637	25.21±2.29	27.81±2.14	32.34±2.77	27.33±2.06
NTUA_007	38.0294	23.7574	24.94±1.24	29.53±2.36	33.15±2.60	28.86±1.54
NTUA_008	38.0865	23.8636	21.92±2.83	24.14±2.83	28.20±3.29	23.12±2.16
NTUA_009	38.0011	23.9287	25.60±0.89	29.54±2.15	32.04±2.29	27.44±1.37
NTUA_010	38.0752	23.6707	25.23±1.22	29.71±2.14	34.45±2.29	28.29±2.05

Table 3. Mean water vapor pressure *e* (mbar) and relative humidity *RH* (%) with the corresponding standard deviations (±1σ) for 00:00, 06:00, 12:00 and 18:00 UTC for the period 15-31 July 2009 for 13 stations in the Athens LUZ. For each time, the highest and lowest *e* and *RH* are highlighted with dark and light grey shadow, respectively.

Station	Water vapor pressure (mbar)				Relative humidity (%)			
	00:00	06:00	12:00	18:00	00:00	06:00	12:00	18:00
DUTH_001	14.65±1.95	14.94±1.33	14.15±2.37	14.27±2.60	43.46±4.98	36.66±3.50	29.23±4.48	36.66±4.72
DUTH_002	14.49±2.15	14.31±1.44	13.94±2.06	14.09±2.80	36.15±4.74	34.68±3.28	23.48±3.57	30.88±6.03
DUTH_003	15.26±2.23	15.31±1.35	14.21±2.49	14.45±2.83	44.02±5.43	40.74±3.64	27.81±4.75	36.21±5.25
DUTH_004	14.88±2.21	14.92±1.43	14.14±2.33	14.46±3.05	42.01±5.30	37.80±3.45	26.28±4.14	34.74±6.23
DUTH_005	15.80±3.02	15.80±2.56	15.32±3.88	15.51±4.44	42.08±6.54	38.75±4.97	29.15±7.26	36.37±10.99
DUTH_006	15.12±2.70	15.70±2.51	14.84±3.40	15.27±4.15	39.35±5.86	33.09±4.53	27.73±5.84	35.36±9.42
DUTH_007	14.02±1.85	14.58±1.48	13.54±2.24	13.57±2.40	46.12±6.72	38.48±4.91	28.80±4.64	36.98±5.21
DUTH_OA1	15.50±2.22	15.85±1.32	16.11±2.50	16.18±3.43	49.02±5.91	43.30±3.65	31.88±4.44	39.81±6.30
DUTH_OA2	16.39±2.34	16.96±1.52	17.25±2.60	17.12±3.46	45.17±5.53	43.70±3.71	33.71±4.23	41.10±6.98
DUTH_OA3	14.85±2.16	15.05±1.34	15.33±2.51	15.36±3.20	40.51±5.05	40.28±3.50	30.83±3.95	36.73±6.09
NOA1_001	17.00±2.46	17.46±2.21	17.81±3.43	17.97±4.02	46.37±5.12	40.30±3.91	30.53±6.59	42.73±8.30
NOA2_002	15.48±1.72	16.36±1.56	16.77±2.68	15.43±2.17	53.27±8.60	48.70±6.07	40.83±6.08	49.55±7.09
NOA3_003	14.40±2.28	14.21±1.34	13.47±2.42	14.03±3.29	43.41±6.15	36.34±4.58	27.33±4.58	35.65±6.93

Figure captions

Figure 1. Map of measuring sites used for urban canopy air temperature (Tair) analyses in the Greater Athens Area. For station names, see text. The color scale on the left is for the topography (numbers in m). Image from Google Earth.

Figure 2. Mean diurnal variation of spatial T_{air} features for the Athens area during the THERMOPOLIS 2009 campaign (July 15-31, 2009) as measured in 26 stations. Dots denote the station positions. Time is 00 hrs at the upper left panel. Time proceeds with 1-hr step from left to right and from top to bottom. Note that the maps and accompanying color scale do not represent absolute T_{air} but percent departures from the hourly mean of all stations (see also text).

Figure 3. Mean diurnal variation (15-31.7.2009) of T_{air} at four stations representative of different UHI zones within the AthensLUZ. Top left: Center of the city (Pipinou str.), top right: coast (Elliniko), bottom left: site at the NW of the Athens LUZ basin (Nea Philadelphia), bottom right: NE of the LUZ basin (Pikermi).

Figure 4. Timeseries of T_{air} and concurrent satellite acquisition data (MODIS TERRA and AQUA, AVHRR, ASTER, AATSR) for the pixels corresponding to eight T_{air} ground stations.

Figure 5: The diurnal (at 2:00, 8:00, 14:00 and 20:00) spatial evolution of Athens UHI during sea breeze conditions (15th of July 2009). The wind vectors are also plotted. The color scale at the right of each figure shows the percent departures from the area mean, while the distance between two horizontal lines in the scale corresponds to 2.5 m/s wind velocity. For the hourly evolution of UHI, see movie in *Supplement*. Lower panels: MODIS LST at 00:15 (left) and 13:30 (right). Color scale for LST during daytime is 20-55 ^{o}C and during nighttime 10-30 ^{o}C.

Figure 6: The diurnal (at 2:00, 8:00, 14:00 and 20:00) spatial evolution of Athens UHI during Etesian conditions of NE mean synoptic flow (21st of July 2009). The wind vectors are also plotted. The color scale at the right of each figure shows the percent departures from the area mean, while the distance between two horizontal lines in the scale corresponds to 2.5 m/s wind velocity. For the hourly evolution of UHI, see movie in *Supplement*. Lower panels: MODIS LST at 00:15 (left) and 13:30 (right). Color scale for LST during daytime is 20-55 ^{o}C and during nighttime 10-30 ^{o}C.

Figure 7: The diurnal (at 2:00, 8:00, 14:00 and 20:00) spatial evolution of Athens UHI during Etesian conditions of NE mean synoptic flow accompanied by sea breeze conditions, Saharan dust transport and very high temperatures (25th of July 2009). The wind vectors are also plotted. The color scale at the right of each figure shows the percent departures from the area mean, while the distance between two horizontal lines in the scale corresponds to 2.5 m/s wind velocity. For the hourly evolution of UHI, see movie in *Supplement*. Lower panels: MODIS LST at 10:48 (left), 13:30 (middle) and 21:15 (right). Color scale for LST during daytime is 20-55 ^{o}C and during nighttime 10-30 ^{o}C.

Figure 8. Mean diurnal variation of spatial e features for the Athens area during the THERMOPOLIS 2009 campaign (15-31 July, 2009). Dots denote the station positions. Time is 00 hrs at the upper left panel. Time proceeds with 1-hr step from left to right and from top to bottom. Note that the maps and accompanying color scale do not represent absolute e but percent departures from the hourly mean of all stations (see also text).

Figure 9. Mean diurnal variation (15-31.7.2009) of e at four stations within the Athens LUZ. Top left: Center of the city (Pipinou str.), top right: Site at the northeast of LUZ (Marousi), bottom left: site at the south of LUZ (Serifou str.), bottom right: Site at Mt. Penteli.

Figure 10. Comparison of measured and modeled with the UrbClim model mean Tair during the THERMOPOLIS campaign (15-31 July 2009) for the stations deployed within the Athens area.

Figure 11. Mean diurnal variation of spatial T_{air} features for the Athens area during the THERMOPOLIS 2009 campaign (July 15-31, 2009) as modeled by the UrbClim model. Dots denote the station positions. Time is 00 hrs at the upper left panel. Time proceeds with 1-hr step from left to right and from top to bottom. Note that the maps and accompanying color scale do not represent absolute T_{air} but percent departures from the hourly mean of all stations (see also text).

Video 1 (supplement). Variation of spatial T_{air} features for the Athens area during the THERMOPOLIS 2009 campaign (July 15-31, 2009) with 1-hr resolution. Dots denote the station positions. Note that the maps and accompanying color scale do not represent absolute T_{air} but percent departures from the hourly mean of all stations (see also text). Wind velocity and direction vectors are also shown. The color scale at the right of each figure shows the percent departures from the area mean, while the distance between two horizontal lines in the scale corresponds to 2.5 m/s wind velocity.

Figure1

Click here to download high resolution image

Figure2
Click here to download high resolution image

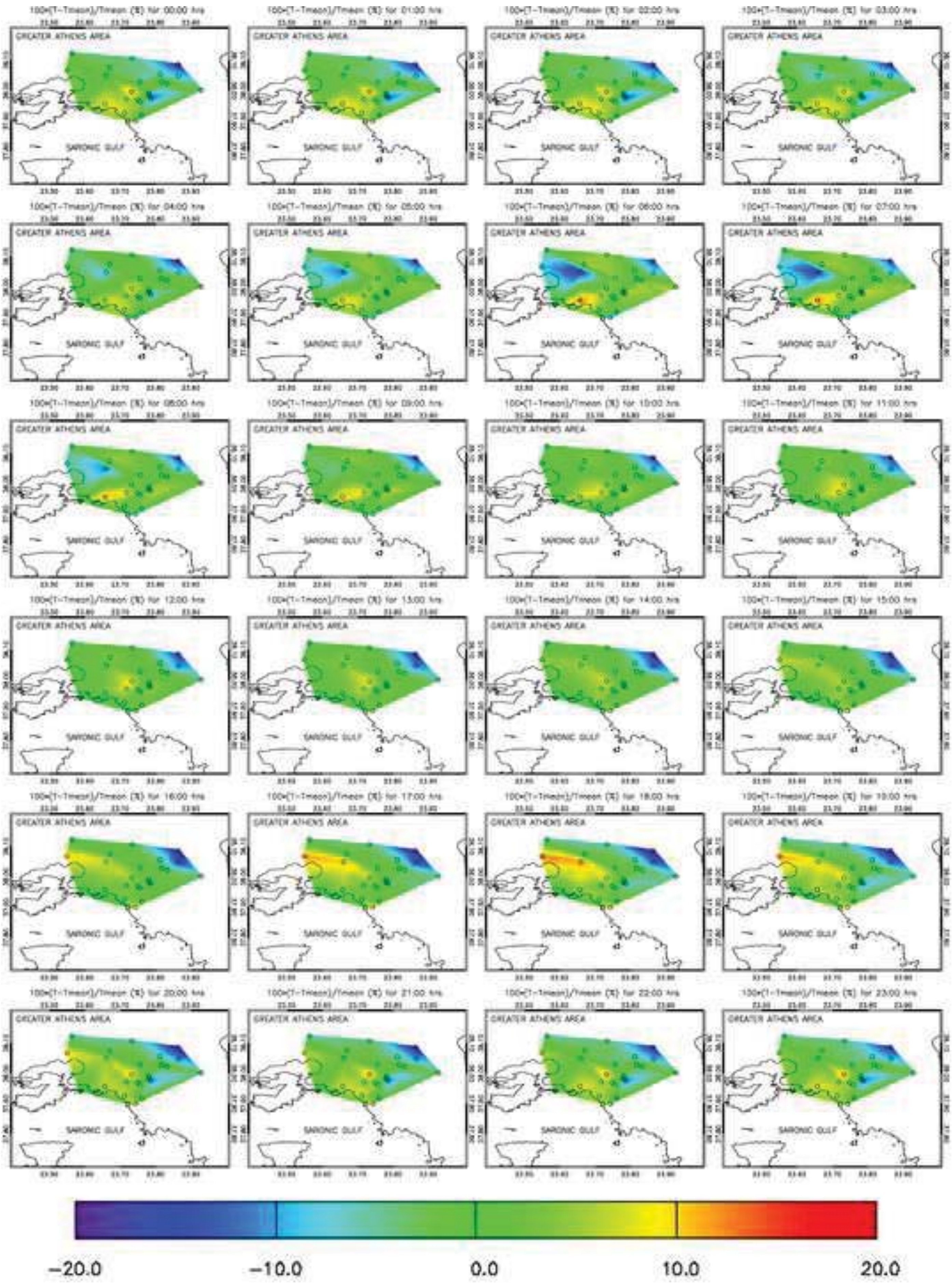

Figure3

Click here to download high resolution image

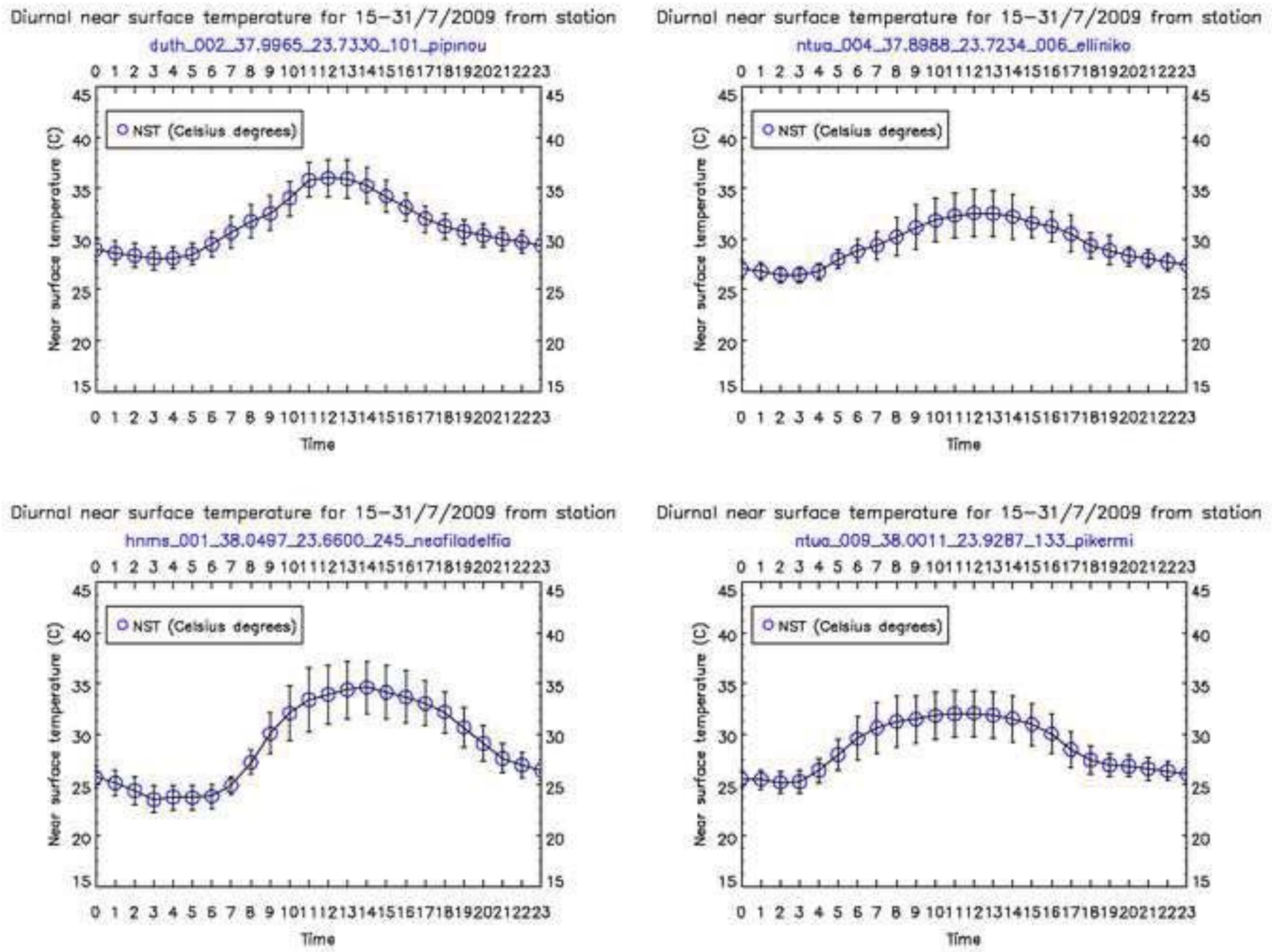

Figure4
Click here to download high resolution image

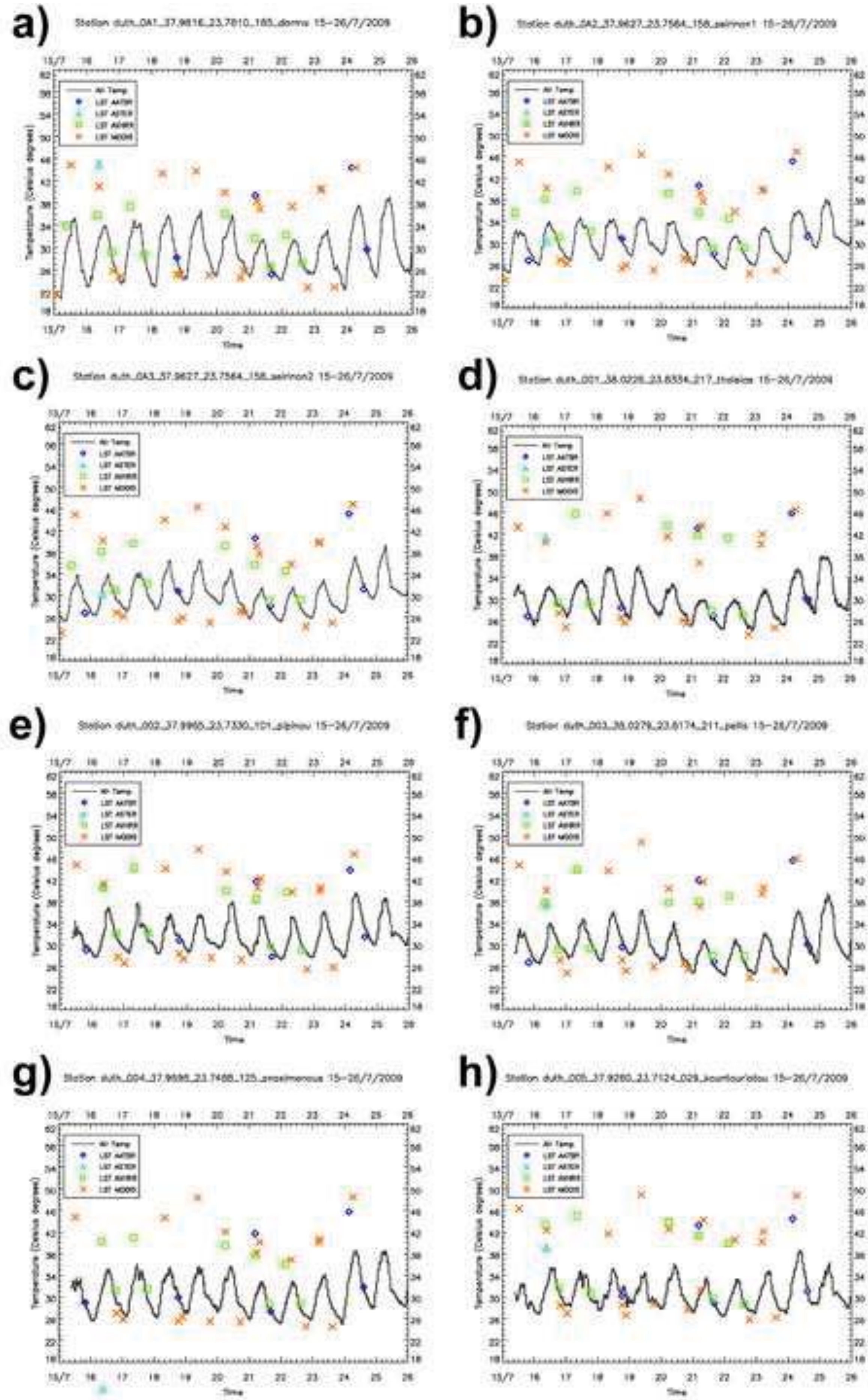

Figure5

Click here to download high resolution image

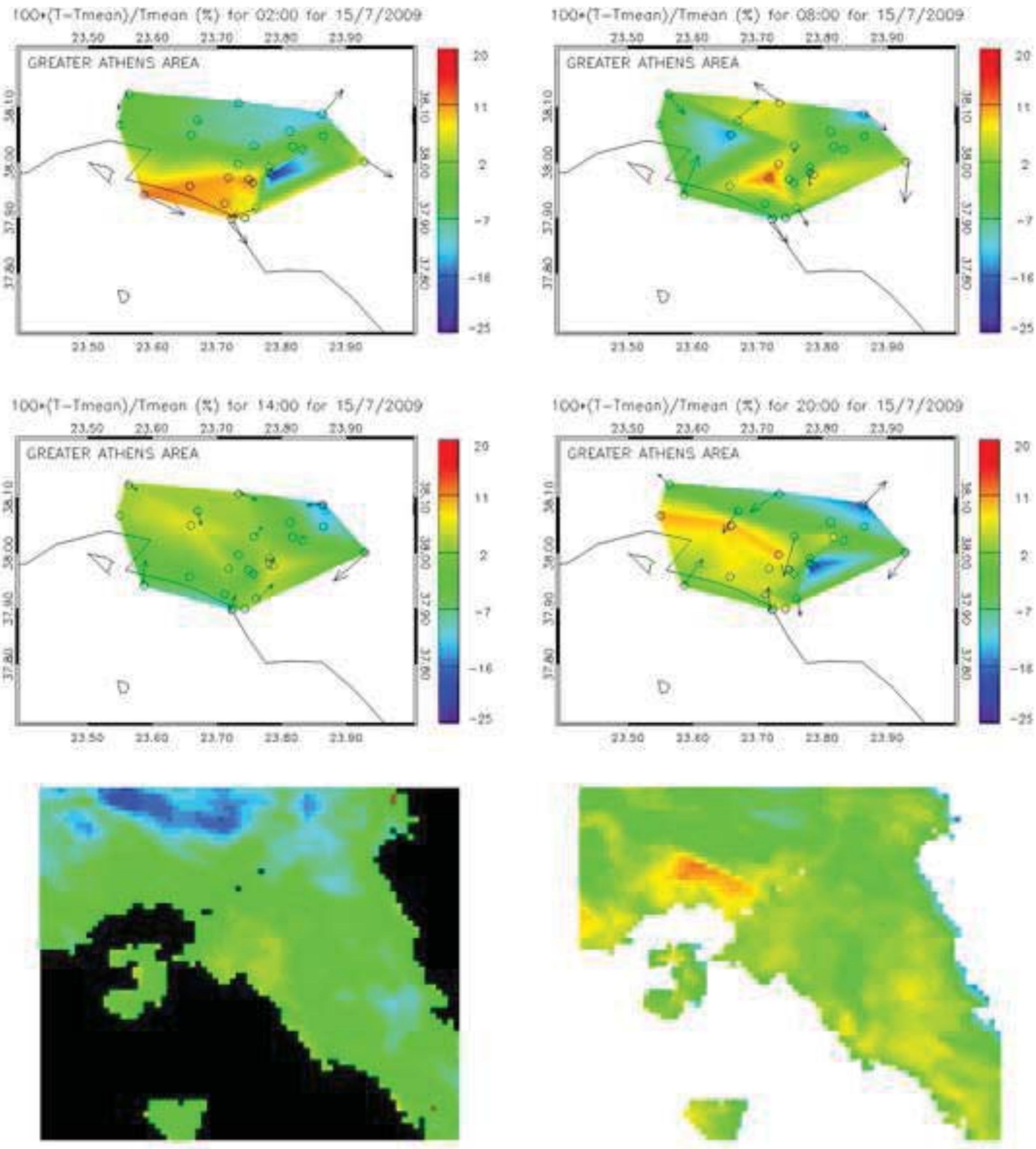

Figure6
Click here to download high resolution image

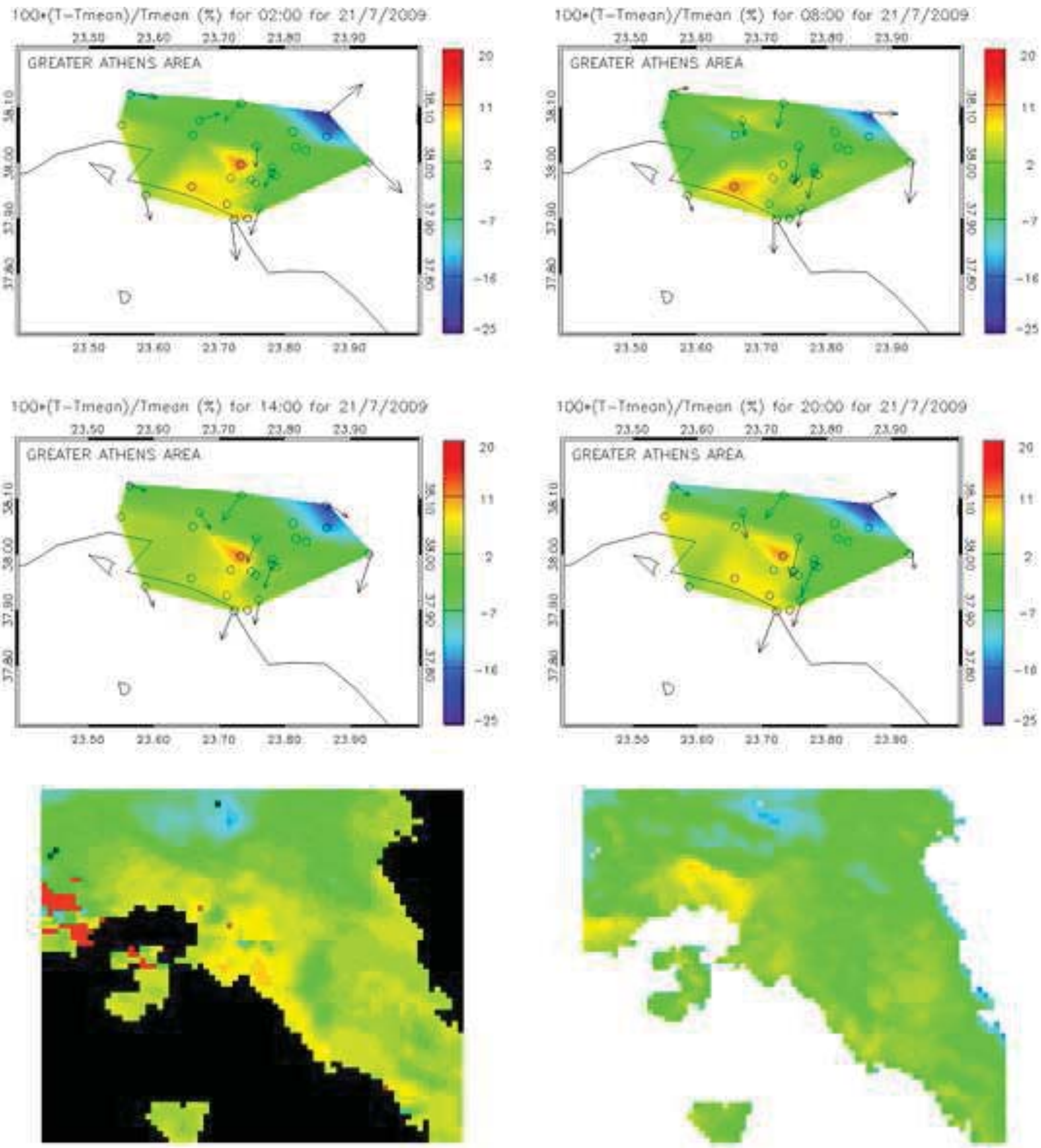

Figure7

Click here to download high resolution image

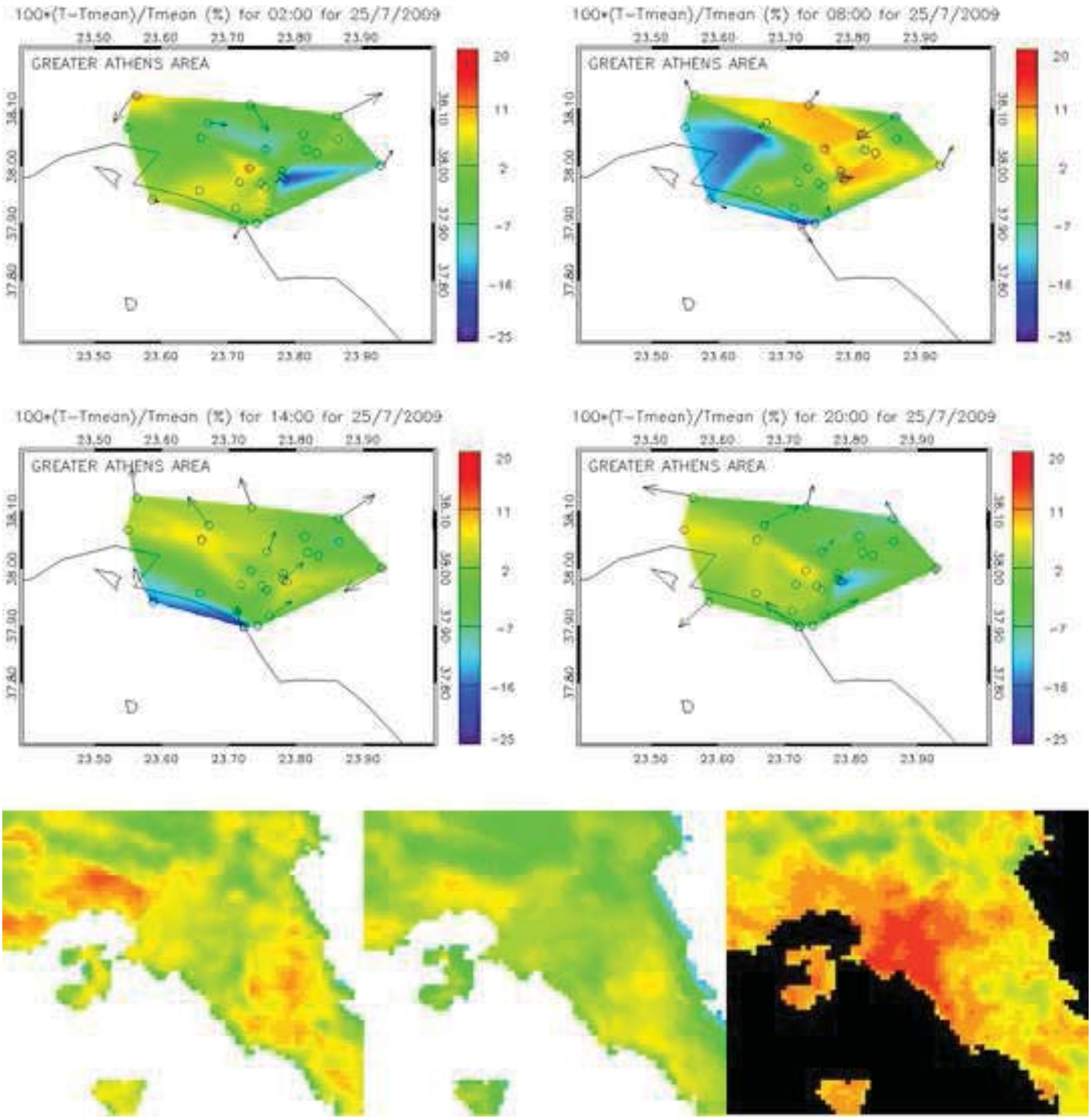

Figure8

Click here to download high resolution image

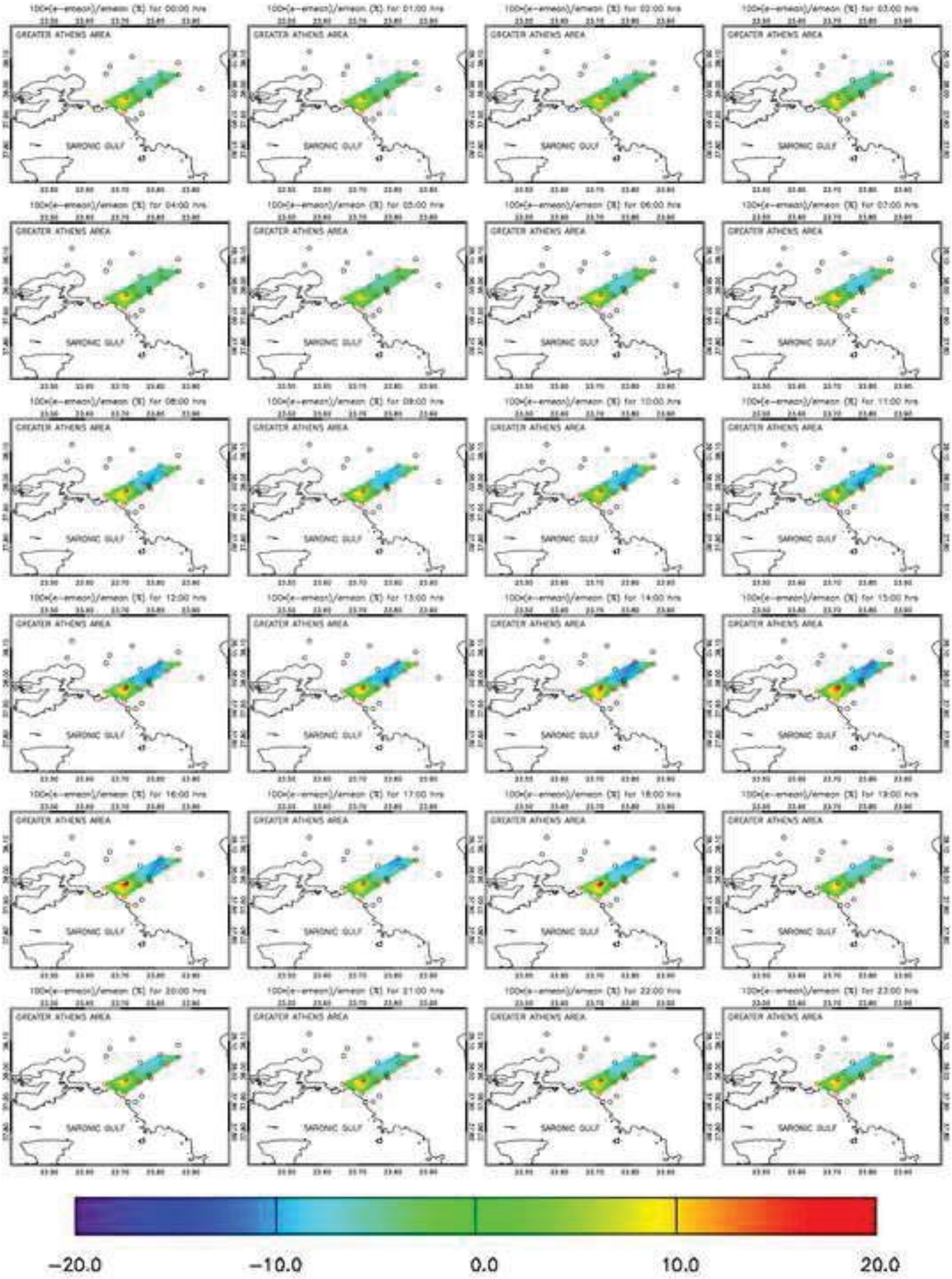

Figure9

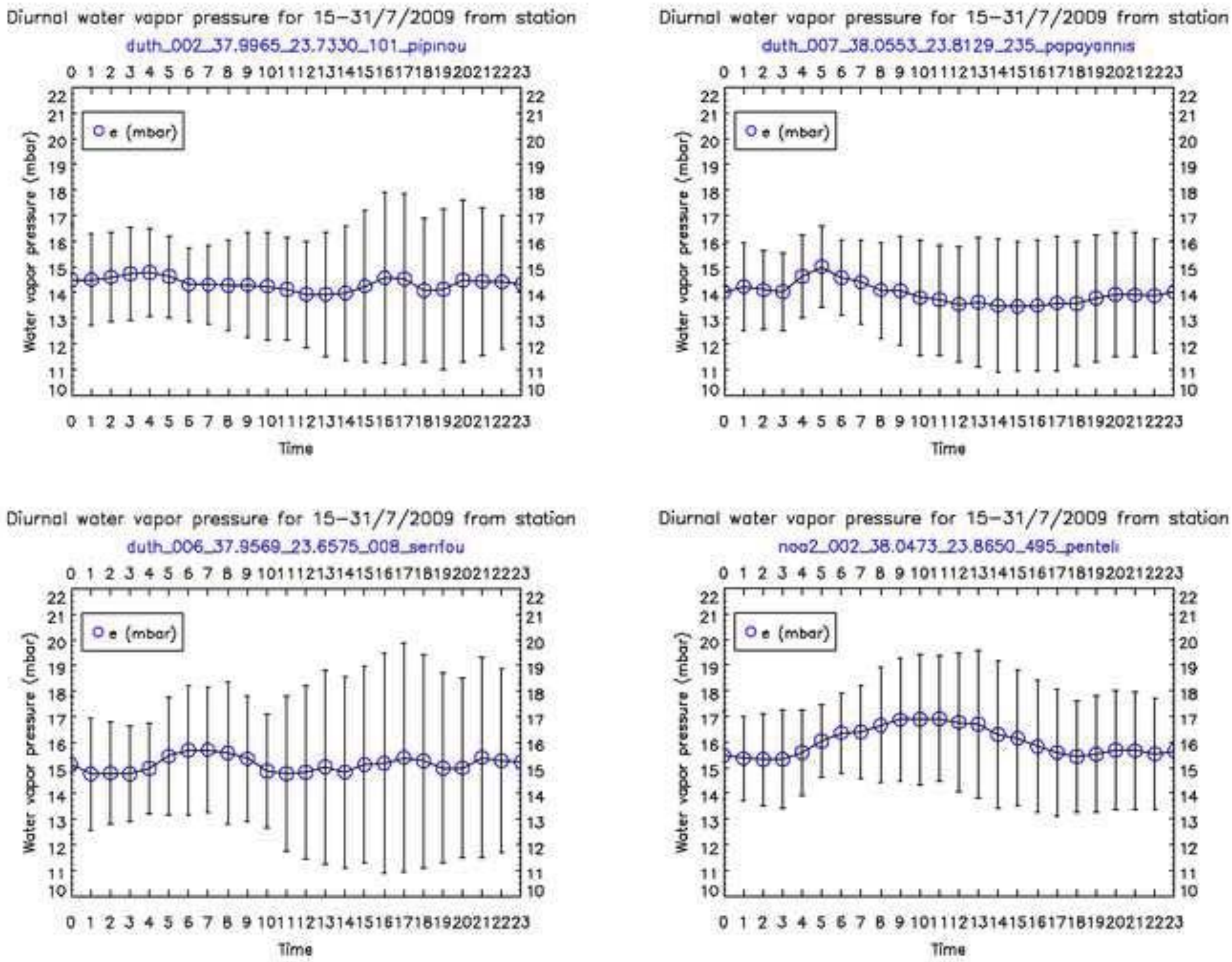
Diurnal water vapor pressure for 15–31/7/2009 from station
duth_002_37.9965_23.7330_101_pipinou
Diurnal water vapor pressure for 15–31/7/2009 from station
duth_007_38.0553_23.8129_235_papayannis
Diurnal water vapor pressure for 15–31/7/2009 from station
duth_006_37.9569_23.6575_008_serifou
Diurnal water vapor pressure for 15–31/7/2009 from station
noa2_002_38.0473_23.8650_495_penteli
e (mbar)
Water vapor pressure (mbar)
Time

Figure10

Click here to download high resolution image

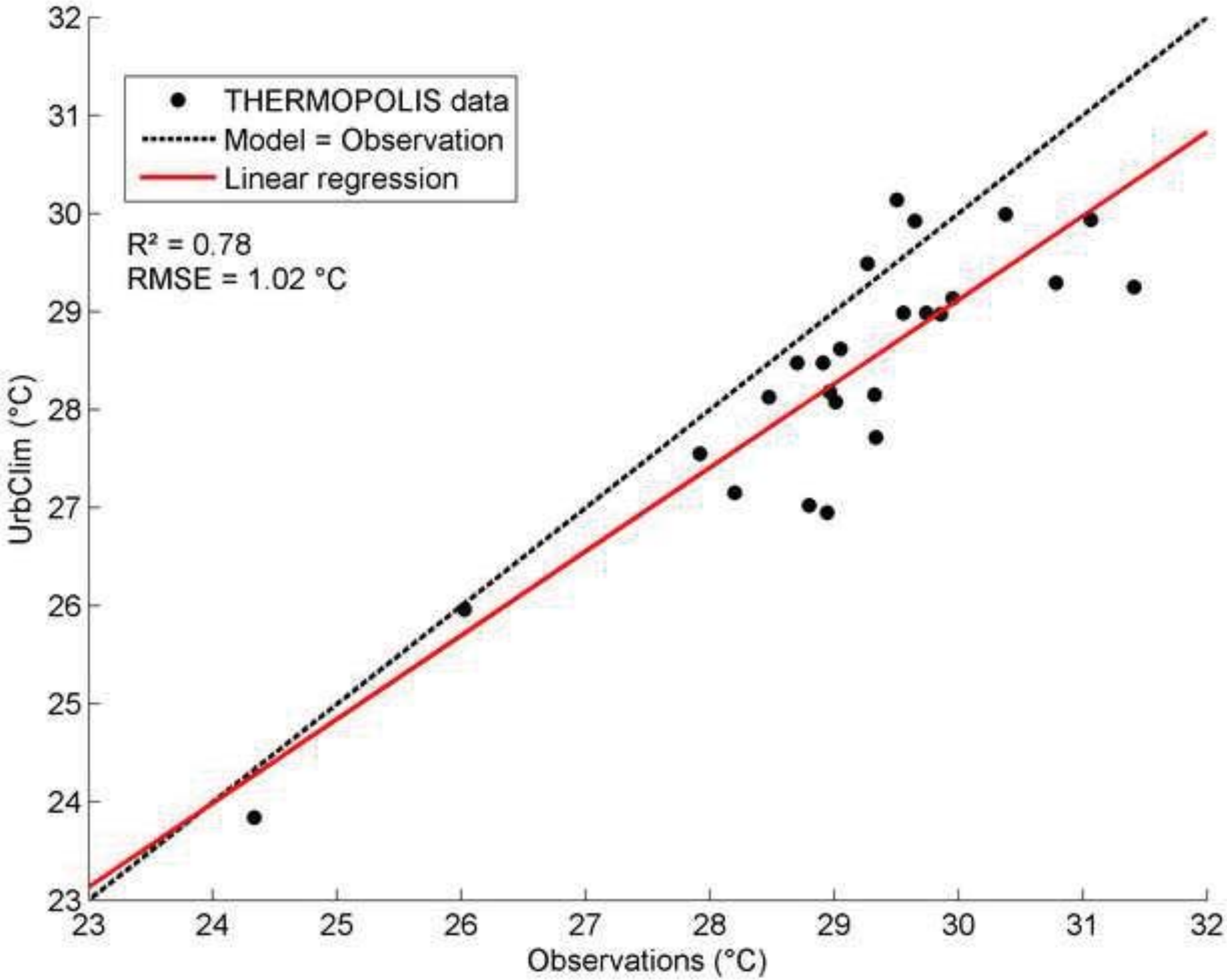

Figure11

Click here to download high resolution image

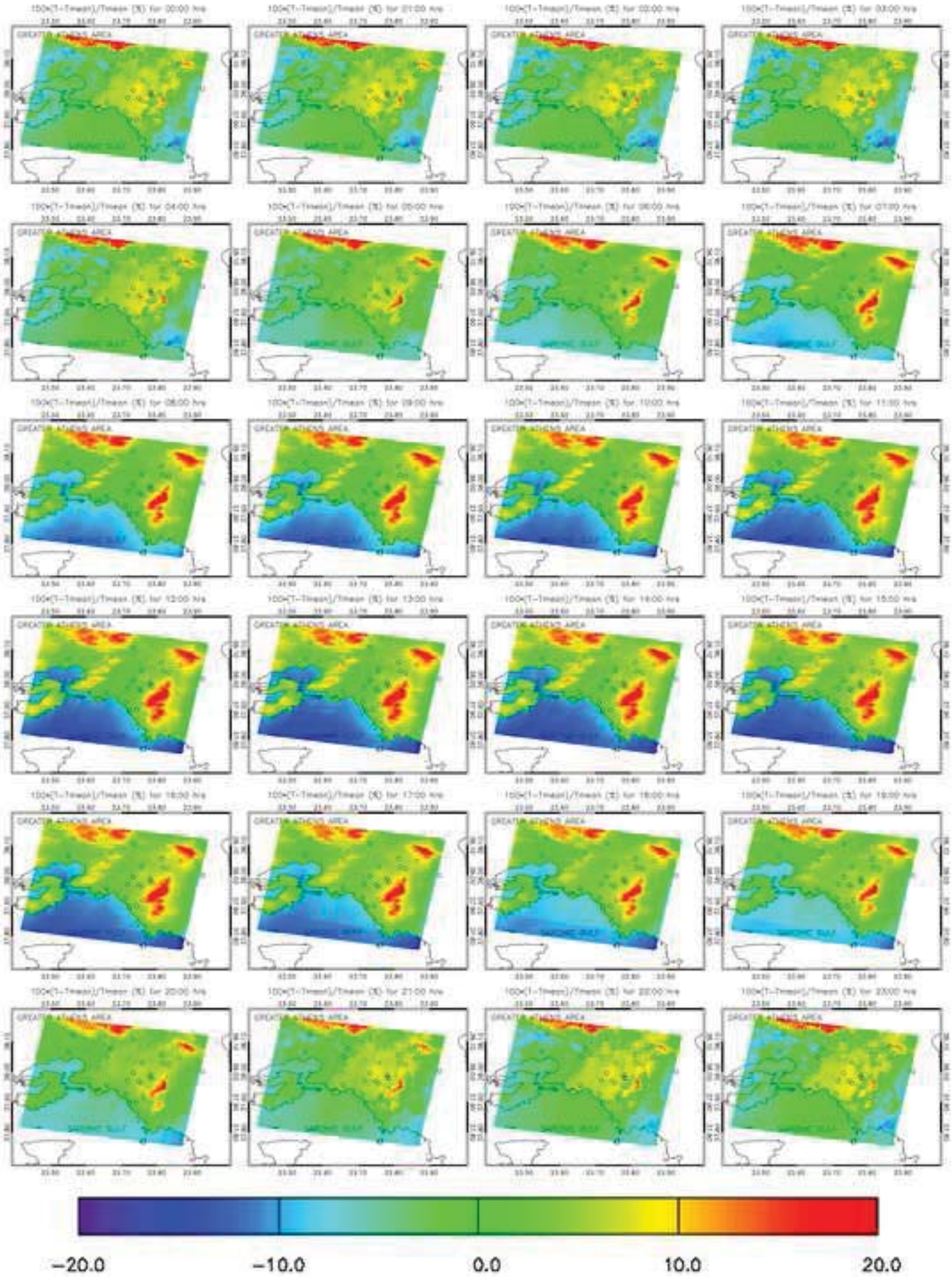

Video
Click here to download Video: Temperature_Athens_Thermopolis-2009.mp4

Video Still
Click here to download high resolution image